Singlet–triplet excitation spectrum of the CO–He complex. I. Potential surfaces and bound–bound CO($a\,^3\Pi \leftarrow X\,^1\Sigma^+$) transitions

W. B. Zeimen, G. C. Groenenboom, and A. van der Avoird
Institute of Theoretical Chemistry, NSRIM, University of Nijmegen, Toernooiveld 1, 6525 ED Nijmegen, The Netherlands

(Received 28 January 2003; accepted 4 April 2003)

The interaction of He with metastable CO($a\,^3\Pi$) gives rise to two adiabatic potential surfaces of reflection symmetry A' and A'' which were calculated with the partially spin-restricted open-shell single and double excitation coupled cluster method with perturbative triples, RCCSD(T). Two diabatic potentials were constructed and fitted analytically; the appropriate form of the angular expansion functions was derived from general invariance properties. From variational calculations on these diabatic potential surfaces we obtained the quasibound vibration-rotation-spin levels of the CO–He complex in its lowest triplet state. Only the lower spin–orbit levels of this complex with approximate quantum number $\Omega=0$ of the CO($a\,^3\Pi$) monomer were found to be stable with respect to dissociation into He and triplet CO. The potential and the bound van der Waals levels of the ground state CO($X\,^1\Sigma^+$)–He complex were recalculated and used in combination with the triplet excited state wave functions to compute the line strengths and the bound–bound part of the singlet–triplet excitation spectrum of the CO–He complex. The spin-forbidden singlet–triplet transitions access mainly the higher spin–orbit levels with $|\Omega|=1$, but these were found to undergo rapid predissociation. The companion Paper II explicitly studies this process, predicts the excited state lifetimes, and generates the bound-continuum part of the CO–He singlet–triplet spectrum. © *2003 American Institute of Physics.* [DOI: 10.1063/1.1577334]

I. INTRODUCTION

The CO molecule is of considerable interest. It plays an important role in interstellar molecular clouds in which collisions occur mostly with abundant species such as He and H_2. The lowest triplet state of CO, the $a\,^3\Pi$ state, is metastable with life times from a few ms to hundreds of ms for the different sublevels of this state.[1,2] This implies that triplet CO molecules are sufficiently long-lived to perform (surface) scattering experiments.[3,4] Since an already cold molecular beam of CO($a\,^3\Pi$) molecules could be decelerated to substantially lower velocity,[5] triplet CO is also a good candidate for the study of ultracold molecules. In view of these prospects it is of interest to study what happens to the metastable CO($a\,^3\Pi$) species when it interacts with other molecules. The simplest possible complex containing CO($a\,^3\Pi$) is the triplet excited van der Waals molecule CO–He, but the first experimental attempts to detect this species were not successful.[6]

The relatively small number of electrons in CO and He allows an accurate theoretical investigation, which is the subject of the present pair of papers. The spin-forbidden $a\,^3\Pi \leftarrow X\,^1\Sigma^+$ transition in the CO monomer gives rise to the so-called Cameron band which was analyzed in detail by spectroscopy.[7,8] Here we study the same transition in the CO–He complex, after characterization of this complex both in its ground and lowest triplet states. The results will show that almost all of the excited triplet CO–He complexes are rapidly destroyed by dissociation. This dissociation does not produce CO in the ground $X\,^1\Sigma^+$ state, however, but in the lower sublevels of the triplet state. In the second paper we will describe how triplet excited CO–He can be detected anyway.

According to the Born–Oppenheimer approximation this theoretical study consists of two steps. The first step involves the calculation of the potential surfaces of the $X\,^1\Sigma^+$ and $a\,^3\Pi$ states of CO interacting with He. The $a\,^3\Pi$ electronic state of CO lies 48 473.2 cm^{-1} above the $X\,^1\Sigma^+$ ground state. In CO–He this $^3\Pi$ state splits into an A' and an A'' component due to reflection symmetry.[9] The spin–orbit coupling in the $a\,^3\Pi$ electronic state of CO makes this state a typical Hund's case (a) system.[10] The spin–orbit coupling constant $A_0=41.45$ cm^{-1} is of the same order of magnitude as the CO–He interaction energy and the spin–orbit coupling turns out to play a crucial role in the dynamics of triplet excited CO–He. The second step is the calculation of the bound and quasibound levels of the ground and triplet excited CO–He complex. We found that rapid photodissociation occurs in most of the excited states, hence the quasibound levels of the triplet species had to be computed by a scattering technique. Dynamical calculations of the triplet states must take the asymptotically degenerate A' and A'' potential surfaces into account simultaneously, and must include the spin–orbit and other coupling terms. Such calculations were performed, after transformation of the adiabatic A' and A'' states to a convenient pair of diabatic states.

The present paper (Paper I) deals with the calculation and the analytic fit of the potential surfaces. Also the calculation of the ground state and triplet excited bound levels in these potentials is described. An effective transition dipole for the spin-forbidden singlet–triplet transition is constructed

TABLE I. Basis set test: interaction energies in μE_h. Calculations with the aug-cc-pVTZ and aug-cc-pVQZ bases also used the 3321 bond functions described in the text.

	aug-cc-pVTZ	aug-cc-pVQZ	Basis of this work
$R=6.770\ a_0,\ \theta=74.150°$			
$X\ ^1\Sigma$	−90.91	−91.36	−91.21
$A'\ ^3\Pi$	−114.56	−115.33	−115.73
$A''\ ^3\Pi$	−100.06	−101.03	−101.02
$R=12.250\ a_0,\ \theta=113.380°$			
$X\ ^1\Sigma$	−3.777	−3.768	−3.815
$A'\ ^3\Pi$	−4.340	−4.337	−4.416
$A''\ ^3\Pi$	−3.855	−3.901	−3.966

and the bound–bound part of the spectrum is generated. The companion paper[11] (Paper II) treats the calculation of the triplet states that dissociate upon excitation.

II. POTENTIAL SURFACES

The CO($X\ ^1\Sigma^+$)–He ground state potential energy surface was calculated previously by Heijmen *et al.*,[12] who used symmetry-adapted perturbation theory (SAPT). Here we applied the CCSD(T) (coupled cluster singles and doubles with perturbative triples) supermolecule method,[13] as we did for the excited triplet state (see below). Since our results for CO($X\ ^1\Sigma^+$)–He agree very well with those of Refs. 12 and 14, we describe in more detail the techniques and calculations involved to obtain the CO($a\ ^3\Pi$)–He potential energy surface. The potentials are expressed in Jacobi coordinates (R,θ) defined such that R is the length of the vector $\mathbf{R}$ which points from the center of mass of CO to the He nucleus and θ is the angle between $\mathbf{R}$ and the CO axis. The angle θ equals zero for the linear geometry CO–He.

A. *Ab initio* calculations

For both the CO($X\ ^1\Sigma^+$)–He ground state and the CO($a\ ^3\Pi$)–He excited state potential surfaces supermolecule calculations were performed with the MOLPRO-2000 package[15] using the CCSD(T) method for the ground state and the partially spin-restricted RCCSD(T) method[16,17] for the excited triplet state. In both cases we applied the counterpoise procedure of Boys and Bernardi[18] to correct for the basis set superposition error (BSSE). We used the same basis set, which consists of $(9s7p3d2f)$ contracted functions defined by Partridge[19] for the C and O atoms and $(5s3p2d)$ contracted functions defined by Van Duijneveldt *et al.*[20] for the He atom. Added to this was a $(3s3p2d1f)$ set of midbond functions defined by Tao and Pan,[21] centered at the midpoint of $\mathbf{R}$, with the exponents 0.9, 0.3, 0.1 for the s and p, 0.6 and 0.2 for the d and 0.3 for the f orbitals. Table I shows that the basis chosen in this work gives results of the same quality as an augmented correlation consistent polarized quadruple zeta (aug-cc-pVQZ) basis.[22–24] The aug-cc-pVQZ basis has 235 contracted functions, whereas the basis used in this work has only 171 (an augmented triple zeta aug-cc-pVTZ basis has 144). It is thus a very good basis for this problem.

For the ground state we used a coordinate grid of 143 points with R ranging from 5 to $9\,a_0$ in steps of $0.5\,a_0$ and from 9 to $12\ a_0$ in steps of $1\ a_0$. The angle θ ranges from 0° to 180° in steps of 15°. The intramolecular CO distance was kept fixed at its equilibrium value $r_e=2.132\ a_0$. For the triplet excited state potential surface the CO bond length was fixed at its $a\ ^3\Pi$ equilibrium value $r_e=2.279\ a_0$ and we calculated 224 points on a coordinate grid with R ranging from 3.25 to $20\,a_0$. The step size was $0.35\,a_0$ in the well region and increases for smaller and larger R. The angular grid ranges from 6° to 174° in steps of 12°.

B. Expansion of the potentials

For the CO–He ground state potential we use the well known Legendre expansion, but the expansion of the A' and A'' potential surfaces that represent the interaction between CO($a\ ^3\Pi$) and He is more complicated. The form of such an expansion for a Π state diatom interacting with an S state atom was first given by Alexander[9] and applied in later work.[25,26] Alexander's derivation of this form is based on the multipole expansion of the interaction energy, which is applicable only for large intermolecular distances and in the case of a neutral S state atom yields an interaction energy that is zero. Here we present a more general derivation, which yields the same result, which is based on the invariance properties of a general intermolecular potential energy operator. We start by defining a partly space-fixed coordinate frame with its z-axis aligned with the CO diatom axis and its xz plane fixed in space, independent of the position of the He atom. The He atom has position vector $\mathbf{R}=(R,\theta,\phi)$ in this frame and the electronic orbital angular momentum of the Π state of CO is $\Lambda=\pm1$. The corresponding components of this Π state, which we call diabatic because they do not depend on the position of the He atom, are denoted by $|\Lambda\rangle$. The intermolecular potential energy operator $\hat{V}$ of this open-shell complex is a linear operator in the vector space spanned by the set of diabatic states and may be expanded as

$$\hat{V}=\sum_{\Lambda_1\Lambda_2}|\Lambda_1\rangle V_{\Lambda_1,\Lambda_2}(R,\theta,\phi)\langle\Lambda_2|. \tag{1}$$

The matrix elements $V_{\Lambda_1,\Lambda_2}=\langle\Lambda_1|\hat{V}|\Lambda_2\rangle$ are the diabatic potentials of CO($a\ ^3\Pi$)–He. Each of these diabatic potentials depends on R, θ, and ϕ and can be expanded in Racah normalized spherical harmonics $C_{lm}(\theta,\phi)$,

$$V_{\Lambda_1,\Lambda_2}(R,\theta,\phi)=\sum_{l,m}v^{l,m}_{\Lambda_1,\Lambda_2}(R)C_{lm}(\theta,\phi). \tag{2}$$

From the invariance of the electronic Hamiltonian of CO–He under rotations of the whole system (electrons and nuclei) it follows that the operator $\hat{V}$ must be invariant in particular to rotations $\hat{R}_z$ about the CO axis. Then, from the transformation properties $\hat{R}_z(\alpha)|\Lambda\rangle=|\Lambda\rangle\exp(-i\Lambda\alpha)$ of the diabatic states and of the spherical harmonics $\hat{R}_z(\alpha)C_{lm}(\theta,\phi)=C_{lm}(\theta,\phi-\alpha)=C_{lm}(\theta,\phi)\exp(-im\alpha)$ it can be easily derived that the expansion coefficients $v^{l,m}_{\Lambda_1,\Lambda_2}(R)$ must vanish except when $m=\Lambda_2-\Lambda_1$. Hence, for the $^3\Pi$ state of CO

with $\Lambda=\pm1$ the expansion is restricted to diagonal terms ($\Lambda_1=\Lambda_2$) with $m=0$ and off-diagonal terms with $m=\pm2$.

Next we define a completely body-fixed frame with the same z-axis and the He atom in the xz plane and consider reflection symmetry with respect to this plane. This frame is related to the partly space-fixed frame by a rotation $\hat{R}_z(\phi)$. The rotated diabatic states are $|\Lambda\rangle'=|\Lambda\rangle\exp(-i\Lambda\phi)$. The reflection σ_{xz} simply acts on these rotated states as $\sigma_{xz}|\Lambda\rangle'=(-1)^{\Lambda}|-\Lambda\rangle'$ and the Π states of CO which are symmetric and antisymmetric with respect to reflection are $|A'\rangle=|+\rangle=(|-1\rangle'-|1\rangle')/\sqrt{2}$ and $|A''\rangle=|-\rangle=i(|-1\rangle'+|1\rangle')/\sqrt{2}$, respectively. These A' and A'' states correspond to the adiabatic states of CO–He obtained in electronic structure calculations. Moreover, it follows from the reflection symmetry that the expansion coefficients of the diabatic potentials in Eq. (2) obey the relation $v^{l,m}_{\Lambda_1,\Lambda_2}(R)=v^{l,-m}_{-\Lambda_1,-\Lambda_2}(R)$ and, hence, that $v^{l,0}_{1,1}(R)=v^{l,0}_{-1,-1}(R)$ and $v^{l,-2}_{1,-1}(R)=v^{l,2}_{-1,1}(R)$. Combining these results one finds that the adiabatic potentials $V_{A'}$ and $V_{A''}$ are related to the (rotated) diabatic potentials as

$$\begin{aligned} V_{A'}&=\langle+|V|+\rangle=V_{1,1}-V_{1,-1},\\ V_{A''}&=\langle-|V|-\rangle=V_{1,1}+V_{1,-1}. \end{aligned} \tag{3}$$

Hence, the diabatic potentials can be directly obtained from the computed adiabatic potentials $V_{A'}$ and $V_{A''}$ and they should be expanded in spherical harmonics with fixed values of $m=\Lambda_2-\Lambda_1$ ($=0$ or ±2),

$$\begin{aligned} V_{1,1}(R,\theta)&=\frac{V_{A'}+V_{A''}}{2}=\sum_l v^{l,0}(R)C_{l,0}(\theta,0),\\ V_{1,-1}(R,\theta)&=\frac{V_{A''}-V_{A'}}{2}=\sum_l v^{l,2}(R)C_{l,2}(\theta,0). \end{aligned} \tag{4}$$

The ϕ dependence in Eq. (2) is automatically removed by the rotation $\hat{R}_z(\phi)$ of the diabatic states and the condition $m=\Lambda_2-\Lambda_1$. So, finally, the diabatic potentials depend only on the coordinates R and θ defined by the nuclear framework. The spherical harmonics $C_{l,m}(\theta,0)$ are simply associated Legendre functions $P^m_l(\theta)$, multiplied by a normalization constant. The same expansion, with $m=0$, holds for the potential of ground state CO($X\,^1\Sigma^+$)–He.

C. Analytic fits of the potentials

The preceding section shows that the angular dependence of the potential of ground state CO($X\,^1\Sigma^+$)–He and of the two diabatic potentials for CO($a\,^3\Pi$)–He can be represented by a specific series of spherical harmonics $C_{l,m}(\theta,0)$ with fixed $m=0$ or ±2 and $|m|\leqslant l<\infty$. Here we describe the analytic fit of each of these potential surfaces in terms of these functions $C_{l,m}(\theta,0)$ and an appropriate set of radial functions that represent both the long and short range interactions,

$$V(R,\theta)=V_{\rm sr}(R,\theta)+V_{\rm lr}(R,\theta), \tag{5}$$

where

$$V_{\rm sr}(R,\theta)=\sum_{p=0}^{p_{\max}}\sum_{l=m}^{l_{\max}} s_{lp}R^p\exp(-\alpha R)C_{lm}(\theta,0) \tag{6}$$

and

$$V_{\rm lr}(R,\theta)=\sum_{n=6}^{n_{\max}}\sum_{l=m}^{l_{\max}} f_n(\beta R)c_{ln}R^{-n}C_{lm}(\theta,0). \tag{7}$$

The long range coefficients c_{ln} are nonzero only when $l\leqslant n-4$, while l must be even for even n and odd for odd n. The functions f_n are Tang–Toennies damping functions,[27]

$$f_n(x)=1-\exp(-x)\sum_{k=0}^{n}\frac{x^k}{k!}. \tag{8}$$

The coefficients s_{lp} and c_{ln} and the nonlinear parameters α and β were fit in a two-step procedure.[28] In the first step we fitted the long range data points, i.e., the interaction energies for $R>10\,a_0$, using only the $n=6$, 7, 8, 9 terms of the expansion function $V_{\rm lr}$ with the damping function set to one. In this step the coefficients c_{ln} were determined by a weighted least squares fit using the weight function $w(R)=R^6$. In the second step we included also the short range data points, we fixed the coefficients c_{ln} with $n=6$, and determined all other linear coefficients in $V_{\rm lr}$ and $V_{\rm sr}$ by a least squares procedure. Since, for the range of R that we considered, the interaction energies vary over several orders of magnitude we had to construct a weight function $w(R,\theta)$ such that $w(R,\theta)V(R,\theta)$ is on the order of unity everywhere. Both in the short and long range $w=|V|^{-1}$ would actually work well, but in the intermediate range the interaction potential goes through zero. Following Ref. 28 we used the weight function $\omega=\omega_{\rm sr}\omega_{\rm lr}$ with

$$\begin{aligned} \omega_{\rm sr}&=\left[\ln\left\{\exp\left(\frac{V}{V_0}\right)+\mathrm{e}-1\right\}\right]^{-1},\\ \omega_{\rm lr}&=\left[1+\left(\frac{R}{R_0}\right)^6\right]V_0^{-1}, \end{aligned} \tag{9}$$

and $V_0=c_6/R_0^6$. This parameter V_0 determines where the short range factor of the weight function effectively "switches on." We set it equal to $V_0=5|E_0|$, where $E_0=-21.29\ \mathrm{cm}^{-1}$ for the ground state potential and $E_0=-27.52\ \mathrm{cm}^{-1}$ for the triplet state potentials are the most attractive points on the grid. The value of $c_6=11.8\,E_{\rm h}a_0^6$ was taken from the long range fit result; it gives $R_0=5.16\,a_0$.

The nonlinear parameters α and β, as well as the upper limits $p_{\max}$ and $n_{\max}$ in the summations (i.e., the degrees of the polynomials), were determined by extensive experimentation. The quality of the fit was judged by considering the relative error for points where $V>V_0$, the absolute error for points with $V<0$, and the relative error for points with $R>7\,a_0$. This test was done not only for the geometries mentioned before, but also for 15 additional random geometries in the range $4\,a_0<R<14\,a_0$ that were not used in the fit. The nonlinear parameters α and β were determined in fits with only low degree polynomials. Once a reasonably good fit was obtained, the nonlinear parameters were fixed and the order of the polynomials was increased step by step as long as this produced a substantial improvement of the fit.

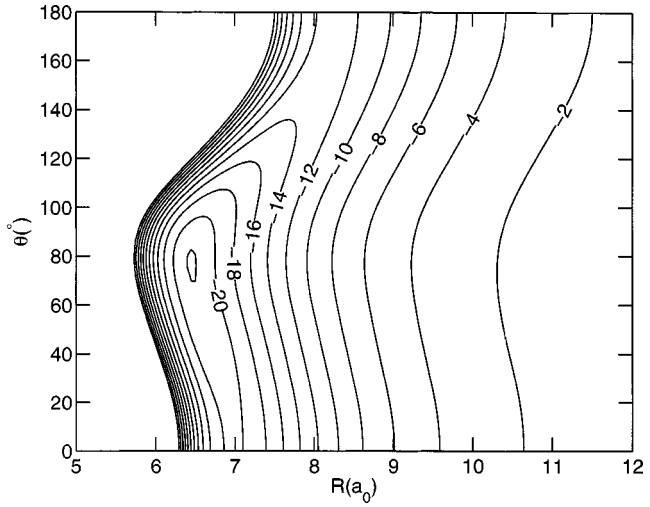

FIG. 1. Potential energy surface of CO($X\,^1\Sigma^+$)–He.

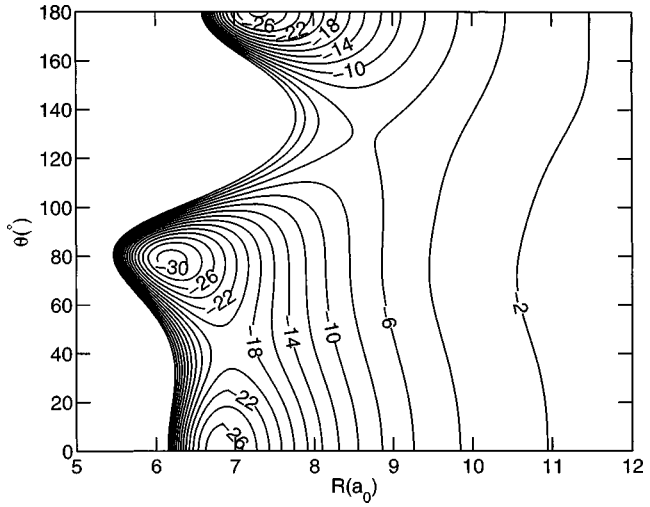

FIG. 2. Adiabatic potential energy surface of CO($a\,^3\Pi$)–He of A' symmetry.

Our final fit for the CO($X\,^1\Sigma^+$)–He potential (with $m=0$) has $p_{\max}=1$, $l_{\max}=10$, and $n_{\max}=14$. The root mean square relative error in the short-range region with $V>0$ is about 0.13%, the root mean square error for the intermediate region with $V<0$ and $R<7\,a_0$ is 0.04 cm^{-1}, and the root mean square relative error in the long range region with $R>7\,a_0$ is 0.8%. For the CO($a\,^3\Pi$)–He potentials the parameters are $p_{\max}=4$, $l_{\max}=9$, and $n_{\max}=13$ for the $V_{1,1}$ surface with $m=0$, and $p_{\max}=8$, $l_{\max}=9$, and $n_{\max}=11$ for the $V_{1,-1}$ surface with $m=2$. For the A' and A'' surfaces that are the sum and difference of $V_{1,1}$ and $V_{1,-1}$ the root mean square relative error in the short-range region is 0.26%, the root mean square error in the intermediate region is 0.03 cm^{-1}, and the root mean square relative error in the long range region is 0.24%.

D. Characteristics of the potentials

Figure 1 shows the (R,θ) contour plot of the ground state CO($X\,^1\Sigma^+$)–He potential. This potential has a single minimum with $D_e=21.35\ \mathrm{cm}^{-1}$ at $R_e=6.48\,a_0$ and $\theta=69°$. This result agrees quite well with the SAPT potential in Ref. 12 which has a minimum with $D_e=22.734\ \mathrm{cm}^{-1}$ at $R_e=6.53\,a_0$ and $\theta=48.9°$. The large difference (20°) in the angle θ is explained by the fact that the potential surface in the well region is very flat along the θ coordinate. Figure 1 shows that at $-21\ \mathrm{cm}^{-1}$, i.e., only 0.35 cm^{-1} above the minimum, the width of the well in the θ direction is $\approx 40°$.

Figures 2 and 3 show the A' and A'' potential surfaces of CO($a\,^3\Pi$)–He, respectively. Minima are found with $D_e=30.76\ \mathrm{cm}^{-1}$ at $R_e=6.22\,a_0$ and $\theta=78°$ for the A' surface and $D_e=31.9\ \mathrm{cm}^{-1}$ at $R_e=6.75\,a_0$ and $\theta=135°$ for the A'' surface. The two surfaces exhibit a common local minimum with $D_e=27.44\ \mathrm{cm}^{-1}$ at the linear CO–He geometry with $R=6.82\,a_0$ and $\theta=0°$.

III. CALCULATION OF THE VIBRATION-ROTATION-SPIN LEVELS

Different coordinates and basis sets can be used to calculate the vibration-rotation-tunneling (VRT) levels of van der Waals dimers. In particular, one may choose a space-fixed coordinate frame or various body-fixed frames with the axes fixed by the orientation of the intermolecular vector **R** and/or by the orientation of one of the monomers.[29,30] In the case of ground state CO–He it turned out that a space-fixed frame (SF) is the most convenient, because the quantum numbers J, describing the CO rotation, and L, the end-over-end rotation of the complex, i.e., of the vector **R**, are very nearly conserved.[12] Also for triplet excited CO–He we will use a SF frame with the same quantum numbers J and L, since the well depth and anisotropy of the A' and A'' potentials of CO($a\,^3\Pi$)–He are comparable to those of the ground state CO($X\,^1\Sigma^+$)–He potential. Before we discuss the calculation of the vibration-rotation-spin levels of the triplet excited CO–He complex, we briefly summarize the fine structure of CO in its $a\,^3\Pi$ state.

The fine structure of CO in its $a\,^3\Pi$ state and in some other excited electronic states has been determined in detail by spectroscopy.[7,8] The dominant term that splits the levels

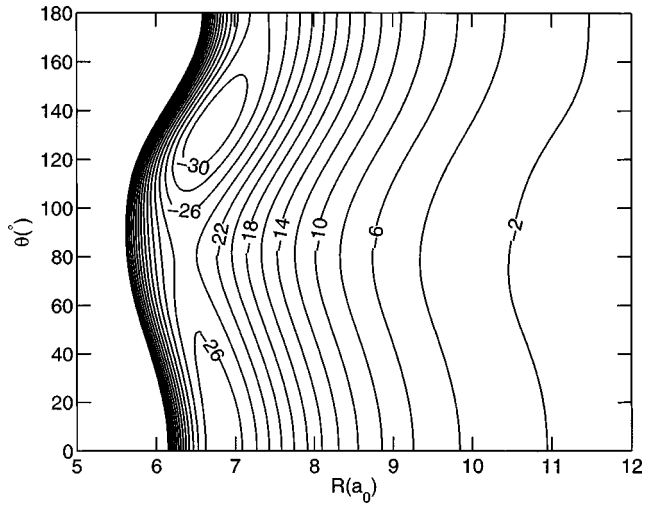

FIG. 3. Adiabatic potential energy surface of CO($a\,^3\Pi$)–He of A'' symmetry.

of CO($a\,^3\Pi$) is the spin–orbit coupling (coupling constant $A_0=41.45\ \mathrm{cm}^{-1}$). The best approximate quantum numbers to characterize these energy levels are $\Lambda=\pm1$ and $\Omega=\Lambda+\Sigma$. The quantum number Λ is the eigenvalue of the electronic orbital angular momentum operator $\hat{l}_z$ and $\Sigma=-1,0,1$, the eigenvalue of $\hat{S}_z$, is the component of the triplet spin ($S=1$) along the CO bond axis. The total angular momentum is represented by the operator $\hat{\boldsymbol{J}}=\hat{\boldsymbol{l}}+\hat{\boldsymbol{S}}+\hat{\boldsymbol{R}}$, where $\hat{\boldsymbol{l}}$, $\hat{\boldsymbol{S}}$, and $\hat{\boldsymbol{R}}$ are the electronic orbital, spin, and nuclear (rotation) angular momenta, respectively. The quantum number J that corresponds with the operator $\hat{\boldsymbol{J}}$ is an exact quantum number. Since the nuclear angular momentum $\hat{\boldsymbol{R}}$ has a vanishing z component Ω is the eigenvalue of $\hat{J}_z$ as well as of the electronic angular momentum operator $\hat{l}_z+\hat{S}_z$. Relative to the origin of the triplet levels at $48\,473.201\ \mathrm{cm}^{-1}$ the levels with $\Omega=0$ are at about $-40\ \mathrm{cm}^{-1}$, the levels with $\Omega=\pm1$ at zero, and the levels with $\Omega=\pm2$ at about $+40\ \mathrm{cm}^{-1}$ as a result of the spin–orbit coupling and CO($a\,^3\Pi$) behaves as a typical Hund's coupling case (a) system. Smaller coupling terms are present as well;[8] the effective Hamiltonian that describes the complete level structure of CO($a\,^3\Pi$) is

$$\hat{H}_{\mathrm{CO}}=B_0[\hat{J}^2+\hat{S}^2-\hat{J}_z^2-\hat{S}_z^2-\hat{J}_-\hat{S}_-+\hat{J}_+\hat{S}_+]+A_0\hat{l}_z\hat{S}_z+\tfrac{2}{3}\lambda_0(3\hat{S}_z^2-\hat{S}^2)+C_\Pi^\delta\hat{P}(\Omega=0), \tag{10}$$

where $B_0=1.6816\ \mathrm{cm}^{-1}$ is the rotational constant of CO($a\,^3\Pi$) in its vibrational ground state, $A_0=41.4500\ \mathrm{cm}^{-1}$ is the spin–orbit coupling constant, $\lambda_0=0.0258\ \mathrm{cm}^{-1}$ the spin–spin coupling constant, and $C_\Pi^\delta=0.8752\ \mathrm{cm}^{-1}$ the Λ-doubling constant. All these coupling constants have been taken from experimental work.[8] Terms smaller than $10^{-2}\ \mathrm{cm}^{-1}$ are omitted. The total angular momentum operator $\hat{\boldsymbol{J}}$ is given with respect to the molecule-fixed frame and its components have the anomalous commutation relations.[31] The corresponding shift operators are therefore defined as $\hat{J}_\pm=\hat{J}_x\mp i\hat{J}_y$, whereas the spin shift operators have the normal definition $\hat{S}_\pm=\hat{S}_x\pm i\hat{S}_y$. The last term in Eq. (10) is the Λ-doubling term which gives rise to a splitting $\mp C_\Pi^\delta$ of the $\Omega=0$ substate into two components with positive and negative parity, see Table IV of Ref. 8. The origin of this splitting is the spin–orbit coupling of the $a\,^3\Pi$ state with other electronic states. The Λ-doubling is represented here by an operator that couples the $|\Lambda=-1,\Sigma=+1\rangle$ and $|\Lambda=+1,\Sigma=-1\rangle$ components of the $\Omega=0$ substate,

$$\hat{P}(\Omega=0)=\sum_{\Lambda=-1,1}|-\Lambda,\Sigma,\Omega=0\rangle\langle\Lambda,-\Sigma,\Omega=0|. \tag{11}$$

For $J>0$ Ω is not an exact quantum number and the substates with $\Omega=\pm1$ and ±2 are slightly split by the Λ-doubling term, due to some admixture of the $\Omega=0$ states.

The Hamiltonian of the triplet excited CO($a\,^3\Pi$)–He complex is easily written now (in atomic units),

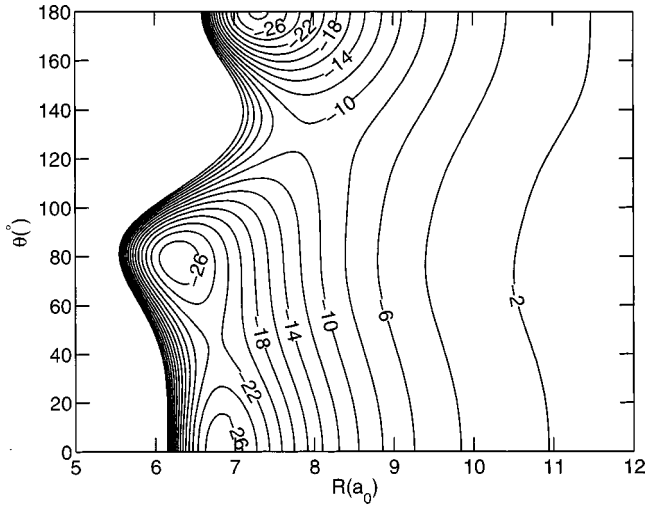

FIG. 4. Diabatic potential energy surface $V_{1,1}$ of CO($a\,^3\Pi$)–He.

$$\hat{H}=\frac{-1}{2\mu R}\frac{\partial^2}{\partial R^2}R+\frac{\hat{L}^2}{2\mu R^2}+\hat{H}_{\mathrm{CO}}+\sum_{\Lambda_1,\Lambda_2}|\Lambda_1\rangle V_{\Lambda_1,\Lambda_2}(R,\theta)\langle\Lambda_2|, \tag{12}$$

where μ is the reduced mass of the dimer and $\hat{\boldsymbol{L}}$ is the angular momentum operator corresponding to the end-over-end rotation. The diabatic potentials $V_{\Lambda_1,\Lambda_2}(R,\theta)$ are defined in Sec. II C and shown in Figs. 4 and 5. The angle θ between the CO bond axis and the vector $\mathbf{R}$ is not one of the SF coordinates, but after the expansion of the potential $V_{\Lambda_1,\Lambda_2}(R,\theta)$ in spherical harmonics given in Sec. II C it is not hard to rewrite this expansion in terms of Wigner D-functions[32] depending on the polar angles of the CO axis and the vector $\mathbf{R}$ with respect to the SF frame. In writing Eq. (12) we assumed implicitly that the weak interaction with He does not change the spin–orbit and spin–spin coupling terms in the Hamiltonian of the CO monomer. A similar Hamiltonian for a Π-state diatom interacting with a rare gas atom has been proposed by Dubernet *et al.*[25]

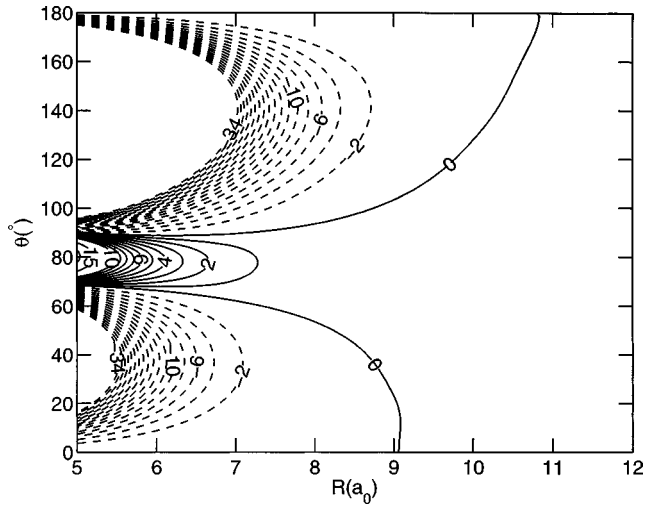

FIG. 5. Diabatic potential energy surface $V_{1,-1}$ of CO($a\,^3\Pi$)–He.

From the discussion on the fine structure of CO in its $a\,^3\Pi$ state it will be clear that the basis functions for this Hund's coupling case (a) system can be denoted as

$$|\Lambda,S,\Omega,J,M_J\rangle = |\Lambda,S,\Omega\rangle \left[\frac{2J+1}{4\pi}\right]^{1/2} D^{(J)}_{M_J,\Omega}(\phi,\theta,0)^*, \tag{13}$$

where the angles (θ,ϕ) are the polar angles of the CO axis with respect to the SF frame. The function $|\Lambda,S,\Omega\rangle$ is the internal (electronic angular momentum and spin) part of the CO($a\,^3\Pi$) wave function (with $S=1$ and $\Sigma=\Omega-\Lambda$) and the symmetric rotor function $D^{(J)}_{M_J,\Omega}(\phi,\theta,0)^*$ describes the CO rotation. From the basis in Eq. (13) we derive a parity adapted basis

$$||\Lambda|,S,\Omega,J,M_J,\epsilon\rangle = 2^{-1/2}[|\Lambda,S,\Omega,J,M_J\rangle + \epsilon(-1)^{J-S}|-\Lambda,S,-\Omega,J,M_J\rangle] \tag{14}$$

consisting of eigenfunctions of the inversion operator with eigenvalues $\epsilon=\pm 1$.

For the CO($a\,^3\Pi$)–He complex we choose the parity-adapted basis

$$|n,|\Lambda|,S,\Omega,J,L;F,M_F,p\rangle = |n\rangle \sum_{M_J,M_L} ||\Lambda|,S,\Omega,J,M_J,\epsilon\rangle Y_{L,M_L}(\beta,\alpha) \times \langle J,M_J;L,M_L|F,M_F\rangle. \tag{15}$$

The angles (β,α) are the polar angles of $\mathbf{R}$ with respect to the SF frame. The triplet CO monomer functions with quantum number J and the spherical harmonics $Y_{L,M_L}(\beta,\alpha)$ have been coupled to eigenfunctions of $\hat{F}^2$ by means of the Clebsch–Gordan coefficients $\langle J,M_J;L,M_L|F,M_F\rangle$.[32] The total angular momentum F, with $\hat{\mathbf{F}}=\hat{\mathbf{J}}+\hat{\mathbf{L}}$, and its SF component M_F are exact quantum numbers. Also the parity p, which is related to the parity ϵ of the monomer functions by $p=\epsilon(-1)^L$, is an exact quantum number. The radial basis functions $|n\rangle=\chi_n(R)$ are Morse oscillator type functions of the form defined in Ref. 33.

The wave functions of ground state CO–He are also given by Eq. (15), but since $\Lambda=S=\Sigma=\Omega=0$ in this case they are much simpler than the wave functions of the triplet state. They are parity-adapted automatically with parity $p=(-1)^{J+L}$. Also the dimer Hamiltonian of Eq. (12) is much simpler: the CO monomer term is $\hat{H}_{\rm CO}=B_0\hat{J}^2$ with $B_0=1.9225\ \mathrm{cm}^{-1}$ and the potential energy operator is $\hat{V}=V(R,\theta)$.

The matrix elements of the Hamiltonian in Eqs. (10) and (12) over the CO($a\,^3\Pi$)–He basis are

$$\begin{aligned}\langle n',\Lambda',S',\Omega',J',L'|H|n,\Lambda,S,\Omega,J,L\rangle &= \delta_{\Lambda',\Lambda}\delta_{S',S}\delta_{\Omega',\Omega}\delta_{J',J}\delta_{L',L}\left[\langle n'|\frac{-1}{2\mu R}\frac{\partial^2}{\partial R^2}R+\frac{L(L+1)}{2\mu R^2}|n\rangle+\delta_{n',n}\left\{B_0[J(J+1)+S(S+1)\right.\right.\\ &\left.\left.-\Omega^2-\Sigma^2]+A_0\Lambda\Sigma+\frac{2}{3}\lambda_0[3\Sigma^2-S(S+1)]\right\}\right]-\delta_{n',n}\delta_{S',S}\delta_{J',J}\delta_{L',L}[\delta_{\Lambda',\Lambda}B_0(\delta_{\Omega',\Omega-1}C^-\\ &+\delta_{\Omega',\Omega+1}C^+)-\delta_{\Omega',\Omega}\delta_{\Omega,0}\delta_{\Lambda',-\Lambda}C^{\delta}_{\Pi}]+\langle n',\Lambda',S',\Omega',J',L'|V_{\Lambda',\Lambda}(R,\theta)|n,\Lambda,S,\Omega,J,L\rangle,\end{aligned} \tag{16}$$

where $\Sigma'=\Omega'-\Lambda'$ and $\Sigma=\Omega-\Lambda$, while $C^{\pm}=[J(J+1)-\Omega(\Omega\pm1)]^{1/2}[S(S+1)-\Sigma(\Sigma\pm1)]^{1/2}$. The primitive (nonparity-adapted) basis $|n,\Lambda,S,\Omega,J,L;F,M_F\rangle$ in these matrix elements is not explicitly defined, but is related to the nonparity-adapted CO momomer basis in Eq. (13) in the same way as the parity-adapted basis in Eq. (15) is related to Eq. (14). The exact quantum numbers F and M_F, which must be equal in bra and ket, are omitted from the notation. The matrix elements of the potential are

$$\begin{aligned}\langle n',\Lambda',S',\Omega',J',L'|V_{\Lambda',\Lambda}(R,\theta)|n,\Lambda,S,\Omega,J,L\rangle &= \delta_{S',S}\delta_{\Sigma',\Sigma}[(2J+1)(2J'+1)(2L+1)(2L'+1)]^{1/2}\\ &\times(-1)^{J'+J+F-\Omega}\sum_l \langle n'|v^{l,\Lambda'-\Lambda}(R)|n\rangle \begin{pmatrix} L' & l & L\\ 0 & 0 & 0\end{pmatrix}\begin{pmatrix} J' & l & J\\ -\Omega' & \Lambda'-\Lambda & \Omega\end{pmatrix}\begin{Bmatrix} J' & L' & F\\ L & J & l\end{Bmatrix}.\end{aligned} \tag{17}$$

The expressions in large round brackets are 3-j symbols, the expression in curly braces is a 6-j symbol.[32]

IV. EFFECTIVE DIPOLE FUNCTION FOR SINGLET–TRIPLET EXCITATION

The spin-forbidden transition $a\,^3\Pi \leftarrow X\,^1\Sigma^+$ has been studied in detail for the free CO monomer.[1,7,8,34] This transition becomes weakly allowed due to mixing of the $a\,^3\Pi$ state with the nearby $A\,^1\Pi$ state induced by the spin–orbit interaction. The transition from the ground $X\,^1\Sigma^+$ state to the $A\,^1\Pi_1$ state is a dipole-allowed perpendicular transition. Since $S=0$ for the $^1\Pi_1$ state, it has only $|\Omega|=|\Lambda|=1$ components and it mixes only with the $|\Omega|=1$ components of the CO($a\,^3\Pi$) state. Effective wave functions for this $|\Omega|$

$=1$ component of the $^3\Pi$ state may be written as $|a\,^3\Pi_{\pm 1}\rangle^{\rm eff}=\sqrt{1-c_{\rm SO}^2}|a\,^3\Pi_{\pm 1}\rangle \pm c_{\rm SO}|A\,^1\Pi_{\pm 1}\rangle$. Hence, only the $|\Omega|=1$ levels of the triplet are directly excited by the $a\,^3\Pi \leftarrow X\,^1\Sigma^+$ transition. In reality, Ω is not an exact quantum number, however, and the substates with different $|\Omega|$ are mixed for nonzero J, so that the $^3\Pi_0$ and $^3\Pi_2$ levels obtain some intensity as well. For low values of J this Ω mixing is small and the transition occurs predominantly to the $^3\Pi_1$ levels.

With this knowledge it is possible to write an effective transition dipole moment for the $a\,^3\Pi \leftarrow X\,^1\Sigma^+$ transition in CO,

$$\begin{aligned}\mu_k^{\rm trans}&=\langle a\,^3\Pi_\Omega|\mu_k|X\,^1\Sigma^+\rangle^{\rm eff}\\&=\delta_{\Omega,\pm 1}\langle\sqrt{1-c_{\rm SO}^2}a\,^3\Pi_{\pm 1}\pm c_{\rm SO}A\,^1\Pi_{\pm 1}|\mu_k|X\,^1\Sigma^+\rangle\\&=\pm c_{\rm SO}\delta_{\Omega,\pm 1}\langle A\,^1\Pi_{\pm 1}|\mu_k|X\,^1\Sigma^+\rangle,\end{aligned}\tag{18}$$

which has only components with $k=\pm 1$ perpendicular to the CO axis. The two matrix elements $\langle A\,^1\Pi_{\pm 1}|\mu_{\pm 1}|X\,^1\Sigma^+\rangle$ are equal and the effective transition dipole moment is here considered to be a known constant $\mu_{\pm 1}^{\rm trans}=\pm\mu_\perp^{\rm trans}$.

We assume that the weak interaction with the He atom does not affect this transition dipole moment. It is the spin selection rule, after all, that makes this transition forbidden, not the spatial symmetry. The closed shell He atom is not expected to affect the spin of the excited CO molecule. The effective singlet–triplet transition dipole function for the CO–He complex is then

$$\mu_m^{\rm SF}=\sum_k \mu_k^{\rm trans}D_{m,k}^{(1)}(\phi,\theta,0)^*.\tag{19}$$

We remind the reader that the angles (θ,ϕ) are the polar angles of the CO axis with respect to the SF frame. The components $m=-1,0,1$ of the dipole function are also defined with respect to this frame.

With the same assumption about the effective CO triplet states we derive for the transition dipole matrix elements $\langle a\,^3\Pi_\Omega|\mu^{\rm SF}|X\,^1\Sigma^+\rangle^{\rm eff}$ over the nonparity-adapted CO–He basis,

$$\begin{aligned}&\langle n',\Lambda,S,\Omega,J',L';F',M_F'|\mu_m^{\rm SF}|n,0,0,0,J,L;F,M_F\rangle\\&\quad=\delta_{n',n}\delta_{L',L}[(2J'+1)(2J+1)(2F+1)(2F'+1)]^{1/2}\\&\qquad\times\sum_{k=-1,1}(-1)^{L+M_F'-k}\mu_k^{\rm trans}\begin{pmatrix}J'&1&J\\-\Omega&k&0\end{pmatrix}\\&\qquad\times\begin{Bmatrix}1&J'&J\\L&F&F'\end{Bmatrix}\begin{pmatrix}F'&1&F\\-M_F'&m&M_F\end{pmatrix}.\end{aligned}\tag{20}$$

A note of caution regarding the parity is needed. It is obvious from Eq. (14) that the transformation of the basis functions under the parity operator involves a phase factor $(-1)^S$. The effective singlet–triplet transition dipole moment function is determined by the admixture of an excited singlet Π state into the triplet Π state considered. This admixture is caused by spin–orbit coupling and was represented in the effective triplet wave functions as $\sqrt{1-c_{\rm SO}^2}|a\,^3\Pi_{\pm 1}\rangle\pm c_{\rm SO}|A\,^1\Pi_{\pm 1}\rangle$. In the basis functions of Eq. (14) the sign of Λ, Ω, and Σ is changed when the parity operator acts upon them, but in addition the triplet $(S=1)$ and singlet $(S=0)$ functions obtain a different sign because of the phase factor $(-1)^{J-S}$. Therefore, parity requires a $\pm$ sign in front of the coefficient $c_{\rm SO}$, which corresponds to the sign of Ω. With the parity-adapted basis of Eq. (14) this ensures that mixing of the singlet and triplet Π functions occurs only when they have the same parity. The parity of the ground state CO–He basis functions is given by $(-1)^{J+L}$. The dipole moment function $\mu_m^{\rm SF}$ has odd parity and, hence, the parity of the excited singlet and triplet Π levels must be opposite to the parity of the singlet ground state level.

From the transition dipole moments we calculate the line strengths

$$S(f\leftarrow i)=\sum_{M_F',m,M_F}|\langle f;F',M_F'|\mu_m^{\rm SF}|i;F,M_F\rangle|^2,\tag{21}$$

where

$$\begin{aligned}|i;F,M_F\rangle&=\sum_{n,J,L}|n,0,0,0,J,L;F,M_F\rangle c_{n,J,L}^{i,F},\\|f;F',M_F'\rangle&=\sum_{n',\Lambda,\Omega,J',L'}|n',\Lambda,S,\Omega,J',L';F',M_F'\rangle\\&\quad\times c_{n',\Lambda,\Omega,J',L'}^{f,F'}\end{aligned}\tag{22}$$

are the eigenstates of the ground state and triplet excited CO–He complex, respectively, expanded in the basis of Eq. (15). Substitution of Eq. (20) into this line strength expression yields

$$\begin{aligned}S(f\leftarrow i)&=(2F'+1)(2F+1)\\&\quad\times\Bigg|\sum_{n',n}\sum_{L',L}\sum_{J',J}\sum_{\Lambda,\Omega}c_{n',\Lambda,\Omega,J',L'}^{f,F'}c_{n,J,L}^{i,F}\delta_{n',n}\delta_{L',L}\\&\quad\times[(2J'+1)(2J+1)]^{1/2}\sum_{k=-1,1}(-1)^{L-k}\\&\quad\times\mu_k^{\rm trans}\begin{pmatrix}J'&1&J\\-\Omega&k&0\end{pmatrix}\begin{Bmatrix}1&J'&J\\L&F&F'\end{Bmatrix}\Bigg|^2.\end{aligned}\tag{23}$$

The $6-j$ coefficient gives the selection rule $\Delta F=0,\pm 1$. Approximate selection rules that hold for the approximate quantum numbers J and L of the ground and excited levels are $\Delta J=0,\pm 1$ and $\Delta L=0$. The approximate selection rule that causes mainly the triplet levels with $|\Omega|=1$ to be excited was already discussed above. Also the exact parity selection rule was mentioned above.

V. COMPUTATIONAL PROCEDURE

A Fortran program was written to calculate the vibration-rotation-spin levels of ground state CO$(X\,^1\Sigma)$–He and excited CO$(a\,^3\Pi)$–He by diagonalization of the Hamilton matrix derived in Sec. III with the use of the potential surfaces from Sec. II. Examination of the convergence of both the ground and excited state levels showed that the rotation-spin basis could be truncated at $J_{\rm max}=12$, while L is running over all values allowed by the triangular rule for a given quantum

number F. The radial basis $|n\rangle$ consisted of 15 functions. The nonlinear parameters $R_e = 11.618\ a_0$, $D_e = 14.376\ \text{cm}^{-1}$, and $\omega_e = 9.876\ \text{cm}^{-1}$ in this basis that determine the Morse potential to which it corresponds, were variationally optimized in calculations with smaller basis sets. To avoid a nonorthogonality problem in the computation of the transition dipole moments we used the same basis for ground state CO($X\,^1\Sigma$)–He and excited CO($a\,^3\Pi$)–He. The vibration-rotation-spin levels were calculated for $F=0$, 1, 2, 3, and 4. This provided all the bound states of CO($X\,^1\Sigma$)–He that are occupied at $T=5$ K and all the excited triplet states in the desired energy range that are accessible by transitions from the occupied ground state levels. The temperature of 5 K was chosen after consultation with the experimentalists.[6] The singlet–triplet transition line strengths were computed from the corresponding eigenfunctions with the expressions given in Sec. IV. A Boltzmann distribution was taken over the levels of ground state CO–He and combined with the energies of the ground and excited levels and with the line strengths to generate the spectrum that corresponds to the bound–bound transitions.

VI. RESULTS

Table II lists the bound levels of CO($X\,^1\Sigma^+$)–He. Their energies as well as the contributions of the dominant angular components in the wave functions are in good agreement with the results of Refs. 12 and 35. The energy levels from Refs. 12 and 35 are lower by 0.7–0.8 cm^{-1} because the well in the SAPT potential is deeper by about 1.4 cm^{-1} than the well in the ground state CO($X\,^1\Sigma^+$)–He potential of this paper, but the relative energies agree to within 0.1 cm^{-1}. The bound states of CO($a\,^3\Pi$)–He are listed in Table III. For each bound state we present its energy, the F and p quantum numbers, and the dominant (Ω,J,L) angular function involved in the total wave function. None of the excited CO($a\,^3\Pi$)–He levels is truly bound, of course, but the life times of the $a\,^3\Pi$ levels of free CO are on the order of milliseconds. So we expected in first instance that the levels of the $^3\Pi$ excited CO–He complex are similarly long lived and can be calculated with a bound state program. It turned out that this holds only for the $\Omega=0$ levels, however. As we mentioned already in the discussion of the free CO($a\,^3\Pi$) levels the $|\Omega|=1$ levels are about 40 cm^{-1} above the $\Omega=0$ levels and the $|\Omega|=2$ levels are higher by another 40 cm^{-1}, mainly due to spin–orbit coupling. The same picture holds more or less for the CO($a\,^3\Pi$)–He complex, although there are many more levels due to the van der Waals vibrations and overall rotations of the complex. The wells in the A' and A'' potentials of CO($a\,^3\Pi$)–He are about 30 cm^{-1} deep, not much deeper than the well in the ground state CO($X\,^1\Sigma^+$)–He potential. In the ground state complex there is a large amount of zero-point energy which leads to a dissociation energy D_0 of only about 7 cm^{-1}. Similarly, the D_0 value for the triplet excited complex is about 8 cm^{-1}, relative to the corresponding Ω levels of free CO. This is schematically shown in Fig. 6. Hence, the quasibound levels of the triplet CO–He complex with $|\Omega|=1$ and $|\Omega|=2$ lie in the continuum of the CO–He state with $\Omega=0$. We found that they could not be converged with a bound state program; their energies kept going down upon increase of the radial basis $|n\rangle$. After explicit photodissociation studies, which are presented in Paper II, we concluded that they rapidly predissociate by a spin–orbit coupling mechanism. The dissociation product is not ground state CO($X\,^1\Sigma^+$) but metastable CO($a\,^3\Pi$) in its $\Omega=0$ state. Table III of the present paper contains only the CO($a\,^3\Pi$)–He levels with $\Omega=0$ that are stable with respect to dissociation into He and triplet CO. One clearly observes the Λ-doubling splitting of about 1.75 cm^{-1} between the pairs of levels with opposite parity. Some of the doublets are incomplete, see for example the third row of Table III, because the upper level lies above the dissociation threshold at $-41.45\ \text{cm}^{-1}$. One can also observe in Tables II and III that the van der Waals levels of triplet excited CO–He are somewhat more mixed in J and L by the anisotropic potential than those of ground state CO–

TABLE II. Bound energy levels of CO–He in its $X\,^1\Sigma^+$ ground state.

Quantum numbers		Energy (cm^{-1})		Main character		
F	p	This work	Ref. 12	J	L	
0	1	−5.9742	−6.7879	0	0	91.2%
0	1	−0.7161	−1.4352	1	1	76.2%
1	1	−1.6978	−2.4800	1	1	97.1%
1	−1	−5.4115	−6.2062	0	1	90.9%
1	−1	−1.9781	−2.7704	1	0	86.0%
2	1	−4.2987	−5.0546	0	2	90.4%
2	1	−1.2728	−2.0385	1	1	86.1%
2	−1	−0.5498	−1.2904	1	2	97.3%
3	−1	−2.6645	−3.3596	0	3	90.0%
3	−1	−0.1154	−0.8338	1	2	85.6%
4	1	−0.5635	−1.1719	0	4	90.3%

TABLE III. Bound energy levels of CO–He in its $a\,^3\Pi$ state. The energy of the two parity levels with $J=\Omega=0$ of free CO are $-40.621\ \text{cm}^{-1}$ and $-38.871\ \text{cm}^{-1}$. All energies are relative to the CO triplet band origin at 48 473.201 cm^{-1}.

Quantum numbers			Main character			
F	p	Energy (cm^{-1})	Ω	J	L	
0	1	−48.2872	0	0	0	83.2%
0	−1	−46.5447	0	0	0	83.0%
0	1	−43.0992	0	1	1	76.2%
1	1	−45.9702	0	0	1	81.6%
1	−1	−47.7129	0	0	1	81.7%
1	1	−44.4316	0	1	1	91.7%
1	−1	−42.6912	0	1	1	91.5%
1	1	−42.9302	0	1	0	75.8%
1	−1	−44.6680	0	1	0	75.9%
1	−1	−42.3730	0	1	2	71.4%
2	1	−46.5759	0	0	2	78.7%
2	−1	−44.8327	0	0	2	78.5%
2	1	−43.8515	0	1	1	72.4%
2	−1	−42.1165	0	1	1	72.2%
2	−1	−43.2249	0	1	2	91.6%
3	1	−43.1565	0	0	3	73.7%
3	−1	−44.9002	0	0	3	73.9%
3	−1	−42.5484	0	1	2	67.2%
4	1	−42.7255	0	0	4	67.4%

TABLE IV. Frequencies in cm^{-1} relative to the singlet–triplet band origin of free CO (48 473.201 cm^{-1}) and line strengths $S(f \leftarrow i)$ in units of $0.01(\mu_{\perp}^{trans})^2$ of the $a\,^3\Pi \leftarrow X\,^1\Sigma^+$ transition for even parity $X\,^1\Sigma^+$ states and odd parity $a\,^3\Pi$ states.

Number in Fig. 7	$(F',J',L') \leftarrow (F,J,L)$	ω_{fi}	Line strength
	(1,0,1)←(0,0,0)	−41.7388	0.0325
	(1,1,0)←(0,0,0)	−38.6938	0.3615
	(1,1,1)←(0,0,0)	−36.7171	0.0125
	(1,1,2)←(0,0,0)	−36.3988	0.0190
	(1,0,1)←(0,1,1)	−46.9968	0.0001
	(1,1,0)←(0,1,1)	−43.9518	0.0016
2	(1,1,1)←(0,1,1)	−41.9751	0.1739
	(1,1,2)←(0,1,1)	−41.6569	0.0033
	(0,0,0)←(1,1,1)	−44.8469	0.0297
	(1,0,1)←(1,1,1)	−46.0151	0.0004
	(1,1,0)←(1,1,1)	−42.9702	0.0106
	(1,1,1)←(1,1,1)	−40.9934	0.1493
	(1,1,2)←(1,1,1)	−40.6752	0.0006
	(2,0,2)←(1,1,1)	−43.1349	0.0393
	(2,1,2)←(1,1,1)	−41.5271	0.0156
	(2,1,1)←(1,1,1)	−40.4187	0.2105
	(1,0,1)←(2,0,2)	−43.4142	0.0192
	(1,1,0)←(2,0,2)	−40.3692	0.0400
	(1,1,1)←(2,0,2)	−38.3925	0.0199
	(1,1,2)←(2,0,2)	−38.0743	0.2847
	(1,0,1)←(2,1,1)	−46.4401	0.0020
	(1,1,0)←(2,1,1)	−43.3951	0.0004
	(1,1,1)←(2,1,1)	−41.4184	0.2246
	(1,1,2)←(2,1,1)	−41.1002	0.0280
	(2,0,2)←(2,0,2)	−40.5339	0.0063
5	(2,1,2)←(2,0,2)	−38.9262	0.6908
	(2,1,1)←(2,0,2)	−37.8177	0.0438
	(2,0,2)←(2,1,1)	−43.5599	0.1248
	(2,1,2)←(2,1,1)	−41.9521	0.0030
3	(2,1,1)←(2,1,1)	−40.8436	0.6189
	(3,0,3)←(2,0,2)	−40.6014	0.1956
7	(3,1,2)←(2,0,2)	−38.2496	0.8061
	(3,0,3)←(2,1,1)	−43.6273	0.0000
	(3,1,2)←(2,1,1)	−41.2756	0.0213
	(3,0,3)←(4,0,4)	−44.3366	0.0131
	(3,1,2)←(4,0,4)	−41.9849	0.0257

He. However, this mixing is still sufficiently weak that one can use these approximate quantum numbers as useful labels of the energy levels.

Although the singlet–triplet transition in CO is only allowed by the spin–orbit mixing of the excited $a\,^3\Pi$ state with the $A\,^1\Pi_1$ state and most of the excitation intensity goes into the triplet levels with $|\Omega|=1$, there is also a part of the spectrum that originates from excitations of the levels with $\Omega=0$. These transitions become allowed by admixture of $|\Omega|=1$ basis functions into the levels with predominantly $\Omega=0$. Tables IV and V list the line strengths of the allowed bound–bound transitions of both parities. The frequencies of these transitions are defined as $\omega_{fi}=E_f-E_i$ relative to the band origin at 48 473.201 cm^{-1} of the $a\,^3\Pi \leftarrow X\,^1\Sigma^+$ transition in free CO. The intensities are in units of the effective singlet–triplet transition dipole moment $\mu_{\perp}^{trans}$ squared. We notice that some of the lines do not respect the approximate selection rule $\Delta L=0$. The most intense lines obey this rule, however. This confirms that the CO–He complex behaves as a slightly hindered rotor also in its triplet excited state, in spite of the more complex nature of this state which contains

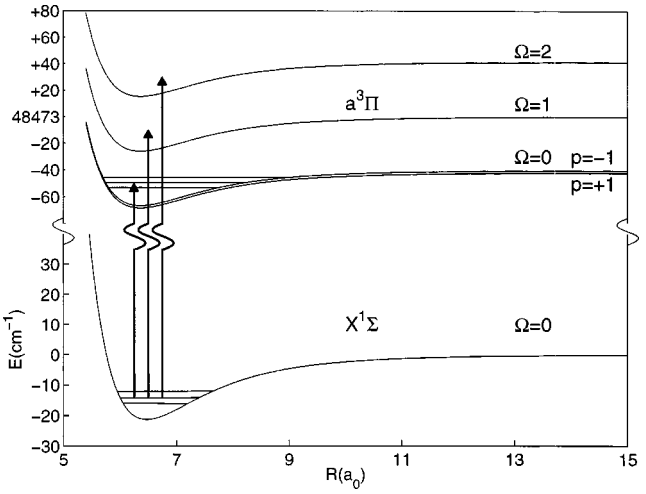

FIG. 6. Schematic energy level structure of ground state $CO(X\,^1\Sigma^+)$–He and UV excited $CO(a\,^3\Pi)$–He at 48 473.201 cm^{-1}.

two diabatic components and a rather anisotropic potential $V_{1,-1}=V_{A''}-V_{A'}$ coupling these components. Figure 7 shows a stick spectrum of this bound–bound part of the spectrum.

VII. CONCLUSIONS

The potential surfaces of the CO–He complex that correspond to the ground $X\,^1\Sigma^+$ state and the excited $a\,^3\Pi$ state

TABLE V. Frequencies in cm^{-1} relative to the singlet–triplet band origin of free CO (48 473.201 cm^{-1}) and line strengths $S(f \leftarrow i)$ in units of $0.01(\mu_{\perp}^{trans})^2$ of the $a\,^3\Pi \leftarrow X\,^1\Sigma^+$ transition for odd parity $X\,^1\Sigma^+$ states and even parity $a\,^3\Pi$ states.

Number in Fig. 7	$(F',J',L') \leftarrow (F,J,L)$	ω_{fi}	Line strength
	(0,0,0)←(1,0,1)	−42.8757	0.0149
	(0,1,1)←(1,0,1)	−37.6877	0.1039
	(0,0,0)←(1,1,0)	−46.3091	0.0008
	(0,1,1)←(1,1,0)	−41.1211	0.0086
	(1,0,1)←(1,0,1)	−40.5587	0.0013
	(1,1,1)←(1,0,1)	−39.0202	0.4137
	(1,1,0)←(1,0,1)	−37.5187	0.0265
	(1,0,1)←(1,1,0)	−43.9921	0.0653
	(1,1,1)←(1,1,0)	−42.4536	0.0062
	(1,1,0)←(1,1,0)	−40.9521	0.4557
	(2,0,2)←(1,0,1)	−41.1644	0.0929
6	(2,1,1)←(1,0,1)	−38.4400	0.6003
	(2,0,2)←(1,1,0)	−44.5978	0.0000
	(2,1,1)←(1,1,0)	−41.8735	0.0136
	(1,0,1)←(2,1,2)	−45.4204	0.0312
	(1,1,1)←(2,1,2)	−43.8818	0.0030
	(1,1,0)←(2,1,2)	−42.3804	0.0356
	(2,0,2)←(2,1,2)	−46.0261	0.0010
	(2,1,1)←(2,1,2)	−43.3017	0.0080
	(3,0,3)←(2,1,2)	−42.6067	0.1066
	(2,0,2)←(3,0,3)	−43.9114	0.0175
	(2,1,1)←(3,0,3)	−41.1871	0.0377
	(2,0,2)←(3,1,2)	−46.4604	0.0030
	(2,1,1)←(3,1,2)	−43.7361	0.0000
	(3,0,3)←(3,0,3)	−40.4920	0.0170
1	(3,0,3)←(3,1,2)	−43.0411	0.2135
4	(4,0,4)←(3,0,3)	−40.0610	0.3567
	(4,0,4)←(3,1,2)	−42.6100	0.0000

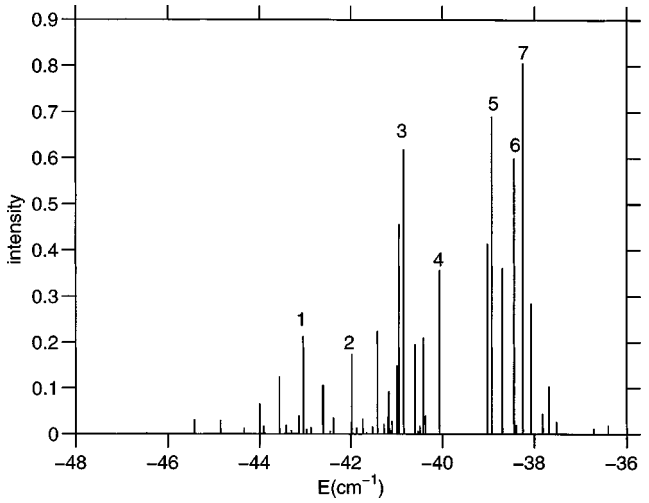

FIG. 7. Theoretical bound–bound spectrum of the $a\,^3\Pi \leftarrow X\,^1\Sigma^+$ transition in CO–He. The frequencies are relative to the band origin ($48\,473.201\ \mathrm{cm}^{-1}$) of the singlet–triplet transition in free CO. Line strength's in units of $0.01(\mu_\perp^{\mathrm{trans}})^2$. For the assignment of the numbered peaks, see Tables IV and V.

of CO were calculated by CCSD(T) methods. The interaction of He with CO($a\,^3\Pi$) gives rise to two potential surfaces which are degenerate at linear geometries of the complex. The van der Waals bound states of the ground and excited state complex were obtained from variational calculations. The bound states of ground state CO($X\,^1\Sigma^+$)–He are in good agreement with earlier studies.[12,35] In the calculation of the bound levels of excited CO($a\,^3\Pi$)–He we used a diabatic representation of the two potential surfaces and the corresponding vibration-rotation-spin basis. Only the lowest spin–orbit levels with $\Omega=0$ were found to be truly metastable quasibound states. Since these states can only decay by de-excitation into the ground singlet state, their life times will be comparable to those of free CO($a\,^3\Pi$). In spite of the more complex nature of the excited state with its two diabatic components coupled by a rather anisotropic potential it behaves as a slightly hindered internal rotor complex, although not quite as weakly hindered as in the ground state.

From the wave functions of the ground and excited state vibration-rotation-spin levels of the complex we computed the line strengths of the singlet–triplet transitions and generated that part of the spectrum that corresponds to excitation of the metastable $\Omega=0$ levels of CO($a\,^3\Pi$)–He. This is only the lower part of the total spectrum, most of the intensity goes into excitation of the triplet levels with $|\Omega|=1$. These levels, and also the still higher spin–orbit levels with $|\Omega|=2$, could not be converged with the bound state program. They couple to the continuum levels of the lowest spin–orbit state with $\Omega=0$ and predissociate. This spin–orbit dissociation mechanism is the subject of Paper II, which describes explicit photodissociation studies. The lifetimes of the quasibound triplet states with $|\Omega|=1$ and $|\Omega|=2$, i.e., the spectral linewidths, and the principal part of the singlet–triplet excitation spectrum of the CO–He complex will be presented in that paper.

ACKNOWLEDGMENTS

This research has been financially supported by the Council for Chemical Sciences of the Netherlands Organization for Scientific Research (CW-NWO). We thank Professor Gerard Meijer for stimulating and useful discussions.

[1] R. T. Jongma, G. Berden, and G. Meijer, J. Chem. Phys. **107**, 7034 (1997).
[2] T. Sykora and C. R. Vidal, J. Chem. Phys. **110**, 6319 (1999).
[3] R. T. Jongma *et al.*, Phys. Rev. Lett. **78**, 1375 (1997).
[4] R. T. Jongma *et al.*, J. Chem. Phys. **107**, 252 (1997).
[5] H. Bethlem, G. Berden, and G. Meijer, Phys. Rev. Lett. **83**, 1558 (1999).
[6] G. Meijer (private communication).
[7] T. James, J. Chem. Phys. **55**, 4118 (1971).
[8] R. Field, S. Tilford, R. Howard, and J. Simmons, J. Mol. Spectrosc. **44**, 347 (1972).
[9] M. H. Alexander, Chem. Phys. **92**, 337 (1985).
[10] G. Herzberg, *Molecular Spectra and Molecular Structure, Vol. 1: Spectra of Diatomic Molecules* (Van Nostrand, New York, 1950).
[11] W. B. Zeimen, G. C. Groenenboom, and A. van der Avoird, J. Chem. Phys. **119**, 141 (2003), following paper.
[12] T. G. A. Heijmen, R. Moszynski, P. E. S. Wormer, and A. van der Avoird, J. Chem. Phys. **107**, 9921 (1997).
[13] J. D. Watts, J. Gauss, and R. J. Bartlett, J. Chem. Phys. **98**, 8718 (1993).
[14] R. Moszynski, T. G. A. Heijmen, and A. van der Avoird, Chem. Phys. Lett. **247**, 440 (1995).
[15] MOLPRO is a package of *ab initio* programs written by H.-J. Werner and P. J. Knowles, with contributions from J. Almlöf, R. D. Amos *et al.*
[16] P. J. Knowles, C. Hampel, and H.-J. Werner, J. Chem. Phys. **99**, 5219 (1993).
[17] P. J. Knowles, C. Hampel, and H.-J. Werner, J. Chem. Phys. **112**, 3106(E) (2000).
[18] S. F. Boys and F. Bernardi, Mol. Phys. **19**, 553 (1970).
[19] H. Partridge, J. Chem. Phys. **90**, 1043 (1989).
[20] J. H. van Lenthe and F. B. van Duijneveldt, J. Chem. Phys. **81**, 3168 (1984).
[21] F. M. Tao and Y. K. Pan, J. Chem. Phys. **97**, 4989 (1992).
[22] T. H. Dunning, Chem. Phys. **90**, 1007 (1989).
[23] R. A. Kendall, T. H. Dunning, and R. J. Harrison, J. Chem. Phys. **96**, 6796 (1992).
[24] D. E. Woon and T. H. Dunning, J. Chem. Phys. **100**, 2975 (1994).
[25] M.-L. Dubernet, D. Flower, and J. M. Hutson, J. Chem. Phys. **94**, 7602 (1991).
[26] M. C. van Beek, J. J. ter Meulen, and M. H. Alexander, J. Chem. Phys. **113**, 628 (2000).
[27] K. T. Tang and J. P. Toennies, J. Chem. Phys. **80**, 3726 (1984).
[28] G. C. Groenenboom and I. M. Struniewicz, J. Chem. Phys. **113**, 9562 (2000).
[29] A. van der Avoird, P. E. S. Wormer, and R. Moszynski, Chem. Rev. **94**, 1931 (1994).
[30] P. E. S. Wormer and A. van der Avoird, Chem. Rev. **100**, 4109 (2000).
[31] R. N. Zare, *Angular Momentum* (Wiley, New York, 1988).
[32] D. M. Brink and G. R. Satchler, *Angular Momentum*, 3rd ed. (Clarendon, Oxford, 1993).
[33] J. Tennyson and B. T. Sutcliffe, J. Chem. Phys. **77**, 4061 (1982).
[34] M. Drabbels, W. L. Meerts, and J. J. ter Meulen, J. Chem. Phys. **99**, 2352 (1993).
[35] R. Moszynski, T. Korona, P. E. S. Wormer, and A. van der Avoird, J. Chem. Phys. **103**, 321 (1995).